RSC Advances

Volume 1 | Number 1 | Jan 2013 | Pages 1–100

RSC Advances

www.rsc.org/advances

ROYAL SOCIETY OF CHEMISTRY

ROYAL SOCIETY OF CHEMISTRY

www.rsc.org/advances

RSC Advances

An international journal to further the chemical sciences

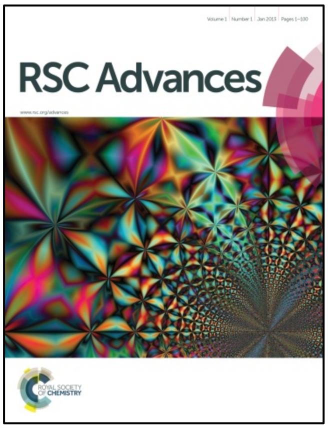

RSC Advances is an international, peer-reviewed, online journal covering all of the chemical sciences, including interdisciplinary fields.

The **criteria for publication** are that the experimental and/ or theoretical **work must be high quality, well conducted adding to the development of the field**.

RSC Advances* has a 2012 partial impact factor of 2.56

Thank you for your assistance in evaluating this manuscript.

Guidelines to the referees

Referees have the responsibility to treat the manuscript as confidential. Please be aware of our Ethical Guidelines, which contain full information on the responsibilities of referees and authors, and our Refereeing Procedure and Policy.

It is essential that all research work reported in *RSC Advances* is well-carried out and well-characterised. There should be enough supporting evidence for the claims made in the manuscript.

When preparing your report, please:

- comment on the originality and scientific reliability of the work;
- comment on the characterisation of the compounds/materials reported - has this has been accurately interpreted and does it support the conclusions of the work;
- state clearly whether you would like to see the article accepted or rejected and give detailed comments (with references, as appropriate) that will both help the Editor to make a decision on the article and the authors to improve it.

Please inform the Editor if:

- there is a conflict of interest
- there is a significant part of the work which you are not able to referee with confidence
- the work, or a significant part of the work, has previously been published
- you believe the work, or a significant part of the work, is currently submitted elsewhere
- the work represents part of an unduly fragmented investigation.

For further information about *RSC Advances*, please visit: www.rsc.org/advances or contact us by email: advances@rsc.org.

*Data based on 2012 Journal Citation Reports®, (Thomson Reuters, 2013).

RSC Advances Accepted Manuscript

Reply to reviewers' comments

Thank you for the reviewers' kind comments. Our incorporation of the reviewers' suggestions is as follows:

Referee #1

1. To make the better arrangement of the paper, the author may consider moving the method of obtaining HPU-g-GO to section 2.3, and the TEM experiments to section 2.4. Besides, more information of TEM experiments should also be provided.

Reply: Thank you for your suggestion. We have moved the preparation of HPU-g-GO in section 2.3 and also explained TEM sample preparation in section 2.4.

2. In Section 2.4, the authors defined shape retention and shape recovery. But this definition is unclear. My understanding of shape retention is the length after unloading divided by the programmed length at high temperature. So it should be L1/(2L0). And the shape recovery ratio should be the final length divided by the initial length which should be L2/L0. The authors need to explain how they define these concepts.

Reply: Thank you for your suggestion. We have modified the explanation for better understanding with addition of references as follows:

The shape memory properties were evaluated by a specimen with a length L_0 was drawn 100 % to $2L_0$ in a temperature controlled chamber at 45 °C and kept at that temperature for 10 min. The specimen under strain was then quenched at 0-5 °C below melting temperature (T_m) of PCL crystals and kept at that temperature for 10 min, and removed the load. The shrunken length (L_1) was measured after the sample had remained at 0-5 °C for 10 min. Shape retention (%) was calculated using equation (1), L_0, and L_1. Finally, the specimen were kept at 60 ^oC above T_m for 10 minutes, and the length (L_2) was measured while the shape change of the samples was recorded using a digital camera. Shape recovery (%) was calculated using equation (2), $2L_0$, and L_2. The shape memory test was repeated three times for each specimen.

The shape recovery was measured by using the following equations (1) and (2).[27,28]

$$\text{Shape retention (\%)} = (L_1 - L_0) / L_0 \times 100 \qquad (1)$$

$$\text{Shape recovery (\%)} = (2L_0 - L_2) / L_0 \times 100 \qquad (2)$$

27. S. S. Mahapatra, S. K. Yadav, H. J. Yoo, M. S. Ramasamy and J. W. Cho, *Sensor. Actuat. B - Chem.,* 2014, **193**, 384-390.

28. B. C. Chun, J. S. Park, C. H. Shin, J. W. Choi and B. C. Chun, *J. Macromol. Res.,* 2012, **20**, 66-75.

3. The paper reports the shape memory performance of the materials. One disadvantage of shape memory polymers is the low mechanical performance in the rubbery state. So lots of shape memory polymer composites are developed to improve the mechanical performance such as large modulus in the rubbery state and force generated during the constrained recovery. This paper has shown the materials are generally stiffer with increasing GO content at low temperature. But actually the readers are generally more interested in the mechanical performance at high temperature especially the mechanical performance at room temperature shows slightly difference. So it would be great helpful if the authors could also provide the stress-strain curve at high temperatures.

Reply: Thank you for your advice. We will keep it in our mind and will present the mechanical performance of shape memory polymer nanocomposite at high temperature in our next communication.

Referee #2

This article developed a new route to prepare graphene oxide reinforced hyperbranched polyurethane. In general, the study is a very interesting work, and the topic is appropriate for the journal “RSC Advances”. The experimental design is appropriate, the results support the conclusions.

Reply: Thank you very much for your comments.

Journal Name RSCPublishing

ICLE

A reactive graphene sheet in-situ functionalized hyperbranched polyurethane for high performance shape memory material

Cite this: DOI: 10.1039/x0xx00000x

Received 00th January 2012,
Accepted 00th January 2012

DOI: 10.1039/x0xx00000x

www.rsc.org/

Sibdas Singha Mahapatra, Madeshwaran Sekkarapatti Ramasamy, Hye Jin Yoo and Jae Whan Cho*

A new and facile route has been developed to prepare graphene oxide (GO) reinforced hyperbranched polyurethane (HPU) composites by in-situ polymerization technique. To increase the reactivity of GO during in-situ polymerization, the aliphatic hydroxyl groups are decorated on the surface of graphene sheets. The enhanced grafting was confirmed by Fourier-transform infrared spectra and high resolution transmission electron microscopy. The high grafting yield of 84 % was obtained from thermogravimetric analysis after removing the non-attached HPU from the composites. The covalently bonded graphene sheets with hyperbranched polyurethane were homogeneously dispersed due to grafted HPU-assisted dispersion in the pure polymer matrix. In comparison with pure hyperbranched polyurethane, the highly flexible graphene-based shape memory polyurethane composite exhibited higher modulus and breaking stress, and exceptional elongation-at-break. The resulting composite exhibited 98 % shape recovery, 93 % shape retention, and enhanced thermal stability; thus, it would be a promising material for the fabrication of graphene-based actuating devices. Consequently, this simple protocol has great potential in the preparation of various high-performance polymer composites.

1. Introduction

Graphene is an ideal two-dimensional material with exceptional structural, chemical, and electrical properties which make it promising candidate in various fields such as polymer composites, microelectronics, photonic devices, and even in biotechnology.[1-3] Especially, the extraordinary properties combined with inexpensive sources (natural graphite) of graphene sheets have encouraged intensive interest in developing high-performance, cost effective polymer composites.[4-6] However, to develop novel composites, it is necessary to produce uniformly dispersed graphene in the polymer matrix. A numerous approaches for preparation and characterization of such composites including melt mixing, in-situ polymerization, and solution casting have been described in several recent reviews.[4,7,8] Both physical and chemical modifications are utilized to increase the solubility and processability and prevent the re-aggregation of graphene, since it can significantly enhance the electrical, physical, mechanical, and barrier properties of polymer composites.[9-11] Noncovalent routes such as π−π stacking and ionic interactions have the advantage to maintain the structural and electrical quality of graphene based materials, however, these structures may be unstable due to relatively weak interactions.[12,13] However, most of these approaches execute below expectation, due to the lack of required reactive functional groups, which are essential for strengthening the interface between the polymer and graphene.

Graphene oxide (GO), derived from the oxidation of graphite, possesses abundant oxygen-containing surface functional groups such as hydroxyls, epoxides, and carboxylic acids which are usually exploited for chemical modification of GO surface.[14] For effective load transfer from polymer to graphene, an approach for controlling the interface between polymer and graphene is necessary. Surface functionalization of GO nanosheets plays a vital role in tailoring the structure and properties of GO and improving the solubility, interaction, and compatibility of GO sheets in polymer systems.[15] Meanwhile, hyperbranched polymers have attracted increasing attention because of their interesting architecture and unique physicochemical properties.[16-19] Firstly, the hyperbranched polymers have a highly branched and non-entangled architecture as well as a large number of terminal groups. The numerous terminal groups can facilitate further modification and reinforce the interactivity with a target polymer by hydrogen bonding or covalent linkage.[20] Secondly, the hyperbranched polymers exhibit much lower melt and solution viscosities and higher solubility in comparison with their linear analogues.[19] However, it is well known that the hyperbranched polymers exhibit inferior mechanical strength due to the lack of entanglement and crystallinity, but this drawback can be overcome by the use of a simple oligomeric diol.[21] To our best knowledge, graphene sheets functionalized with hyperbranched polymers have been seldom reported in the literature.

Meanwhile, enhancing the applications of shape memory polyurethane, researchers have improved its thermal and mechanical properties as well as shape memory properties by incorporating nano-fillers such as carbon nanofibers and carbon nanotubes into the polymer matrix.[22,23] Based on these possibilities, we have already developed conducting polyurethane nanocomposites by incorporating pristine or functionalized carbon nanotubes.[24,25] Although, many research groups have used linear polymer chains to modify the surface of graphene, there are still few reports on highly branched polymers functionalizing the surface of graphene.[4,15,26]

Here, we report a substantially improved approach for the exfoliation of graphene via edge-grafting of three-dimensional hyperbranched macromolecules which are known to show better solubility and large functionality compared with their linear analogues. Thus, the bulky hyperbranched units covalently grafted at the edges of graphene are expected to act as efficient interlocking macromolecular wedges to the polymer matrix and to provide a better mechanical, thermal, and shape memory properties.

2. Experimental

2.1. Materials

GO was purchased from NanoInnova Technologies (Madrid, Spain). 4,4-Methylene bis(phenylisocyanate) (MDI), triethanolamine, thionyl chloride, triethylamine, and dibutyltin dilaurate were purchased from Sigma Aldrich Co (Korea). Poly(ε-caprolactone)diol (PCL, Mw: 3,000 g/mol) was obtained from Solvay (UK). N,N-dimethyl formamide (DMF) was used after purification by conventional technique and stored with 4 Å type molecular sieves.

2.2. Aliphatic hydroxy group functionalization on GO surface

GO containing abundant active acid groups on its basal planes and edges was reacted with excess $SOCl_2$ (20 mL) at 70 °C for 24 h under reflux, and then the residual $SOCl_2$ was removed by distillation under reduced pressure, and further dried under vacuum at room temperature to yield the acyl chloride-functionalized GO. Subsequently, the product was dispersed in 20 mL of anhydrous DMF, and the mixture was sonicated for 30 min in order to create a homogeneous dispersion. The dispersed sample was immediately reacted with 500 mg of tris(hydroxymethyl)-aminomethane in the presence of a catalytic amount of anhydrous triethylamine (TEA, 1 mL) at 0-5 °C for 1 h, further stirred at room temperature for 12 h and finally treated at 70 °C for 12 h under argon atmosphere. The resulting reaction medium was diluted in excess DMF and filtered through a 0.22 μm PTFE membrane. The product was further washed with DMF and acetone for several times and dried at 50 °C under vacuum, and the hydroxyl group functionalized GO (f-GO) was obtained.

2.3. In-situ synthesis of f-GO based hyperbranched polyurethane (NHPU) and pure hyperbranched polyurethane (HPU)

Typically, in a 500 mL four-neck cylindrical vessel equipped with a mechanical stirrer and nitrogen inlet, first the prepolymer was prepared from reaction of 2 g (0.008 mol) 4,4'-methylene bis(phenylisocynate) and 8.1 g (0.0027 mol) poly(ε-caprolactone)diol in 25 mL dry DMF at 70 °C for 3 h. After the completion of prepolymer synthesis, the system was cooled to 0 °C, and the required amounts (Table 1) of THA and f-GO solution in DMF after 15 minute bath sonication were added into the prepolymer solution. The reaction temperature was then increased slowly up to 60 °C and the reaction was allowed to proceed for 3 h under the same conditions. For synthesis of pure HPU, the same procedure was followed but without f-GO (Table 1). After completion of the reaction, the final product solution was dried in a hot air oven at 50 °C to obtain the polymer films with average thickness of 0.4 mm. Different compositions were synthesized by varying the incorporation of second stage f-GO monomer, at 0.5, 1, and 2 wt.%, and the corresponding samples were denoted as NHPU(0.5), NHPU(1) and NHPU(2), respectively. The extent of grafting of GO was analyzed to prepare high dilution DMF solution of NHPU composites and centrifuge to separate pure polymer from hyperbranched grafted GO (HPU-g-GO). The HPU-g-GO powders were obtained by sequential re-dissolving, sonication, and centrifugation with DMF until no turbid mass occurred when the filtrate was added dropwise into water. Dispersion and stability of HPU-g-GO were observed in DMF solution after sonication.

2.4. Characterization

Fourier transform infrared spectroscopic (FT-IR) studies for the samples were recorded in a Jasco FT-IR 300E (Tokyo, Japan) with an attenuated total reflectance method and by using KBr pellets for film and powder samples, respectively. The surface chemical composition of GO and GO-f-TAA was measured by X-ray photoelectron spectroscopy (XPS, ESCSA 2000). ^{1}H-nuclear magnetic resonance (^{1}H-NMR) spectra of the samples were recorded with a Bruker 400-MHz NMR spectrometer by using DMSO-d_6 as a solvent. Differential scanning calorimetry (DSC) measurements were carried out using a TA instrument 2010 (Du Pont) thermal analyzer in a temperature range of -25 °C to 250 °C at a heating rate of 10 °C min^{-1} in nitrogen atmosphere. Thermogravimetric analysis (TGA) was carried out in TA Q50 thermal analyzers, using a nitrogen flow rate of 30 $mLmin^{-1}$ and in room temperature to 700 °C at a heating rate of 10 °C min^{-1}. The graphene nanosheet grafted HPU from pure polymers were separated by dissolving the nanocomposite film in DMF with high dilution and centrifuged washed several time and dried. The functionalization of GO with HPU was analyzed on the basis of their surface morphology using a High resolution transmission electron spectroscopy (HR-TEM, JEM 2100F, JEOL). The HPU-g-GO samples dispersed in DMF solution with sonication and then dropped on 400 mesh copper grids with supporting carbon films were used for TEM measurement.The mechanical properties of the samples were measured at room temperature using a tensile tester machine (Instron 4468). The dimensions of the test specimens were 60×2.9×T mm^3, where T (thickness) is variable. The gauge length and strain rate were 10 mm and 20 mm/min, respectively. In each case, at least five measurements were taken. The shape memory properties were evaluated by a specimen with a length L_0 was drawn 100 % to $2L_0$ in a temperature controlled chamber at 45 °C and kept at that temperature for 10 min. The specimen under strain was then quenched at 0-5 °C bellow melting temperature (T_m) of PCL crystals and kept at that temperature for 10 min, and removal the load. The shrunken length (L_1) was measured after the sample had remained at 0-5 °C for 10 min. Shape retention (%) was calculated using equation (1), L_0, and L_1. Finally, the specimen were kept at 60 °C above T_m for 10 minutes, and the length (L_2) was measured while the shape change of the samples was recorded using a digital camera. Shape recovery (%) was calculated using equation (2), $2L_0$, and L_2. The shape memory test was repeated three times for each specimen. The shape recovery was measured by using the following equations (1) and (2).[27,28]

$$\text{Shape retention (\%)} = (L_1 - L_0) / L_0 \times 100 \qquad (1)$$

$$\text{Shape recovery (\%)} = (2L_0 - L_2) / L_0 \times 100 \qquad (2)$$

3. Results and discussion

The extent of interaction between the polymer and the graphene sheets depends on the level of dispersion of the nanomaterial into the matrix. The homogenous dispersion relies on a method of nanocomposite formation, nature of the polymer, surface functionalities, the degree of modification, and mainly the compatibility between the polymeric matrix and the nanomaterial. Among all the available methods, in-situ polymerization is found to be the best as it leads to the homogenous dispersion of the graphene sheets into the matrix. Herein, the graphene sheets were made to disperse in the hyperbranched polyurethane by in-situ polymerization. The expanded branched structure with large surface functionalities and good compatibility with other systems resulted in excellent interaction and homogenous dispersion of the functionalized graphene sheets with the polymer chains. The schematic procedure and the probable interaction between graphene sheets and HPU are depicted in Scheme 1. This process includes (a) preparation of f-GO through an acylation reaction on the basis of carboxylic groups at GO edges, followed by amidation with tris(hydroxymethyl)-aminomethane to create more reactive aliphatic hydroxyl groups on the GOs surface, and (b) in-situ grafting during hyperbranched polymerization.

The chemical modification of edge-carboxylic acid groups of GO was monitored by acylation with $SOCl_2$ and the substitution reaction with and tris(hydroxymethyl)-aminomethane, respectively. The nature of the chemical groups on the surface of the GO was investigated by the FT-IR spectra shown in Fig. 1a. The main absorption bands of GO at around 1731, 1620, and 3376 cm^{-1} are ascribed to the carboxyl groups, C=C stretching vibration for aromatic ring and the hydroxyl groups, respectively.[15] By the chemical grafting of tris(hydroxymethyl)-aminomethane, the band of GO at 1731 cm^{-1} disappears while a new band at 1697 cm^{-1} assigned to –C=O stretching vibration of amide carbonyl (–CONH–) is observed. Besides, this band at 1545 cm^{-1} (N−H bending vibration of amide) appears in the spectrum. As expected, the bands at 1065 cm^{-1} (C−O−C in epoxide groups) and 3300−3500 cm^{-1} (−OH stretching vibration of hydroxyl groups) still remain in the spectrum of f-GO, indicating that other oxygen-containing functional groups such as epoxide and hydroxyl groups were retained on the surface of f-GO. Furthermore, new peaks corresponding to $–CH_2$ symmetric and asymmetric stretching vibrations appeared at 2926 and 2853 cm^{-1} in f-GO, which confirms the functionalization.

In order to further investigate the structural change of GO after functionalization, XPS analysis of GO and f-GO was performed (Fig. 1b), which demonstrated the presence of C and O in both materials. Two strong peaks at 285.0 eV (C 1s) and 532.0 eV (O 1s) were observed for GO, and f-GO. Moreover, a new but comparatively weak signal was observed at 401.0 eV (N 1s) for f-GO. The relative atomic concentration of nitrogen in f-GO is evaluated to be 3.1 %, authenticating the presence of nitrogenous groups in the sample which confirms the functionalization of tris(hydroxymethyl)-aminomethane via amidation.

The synthesis of hyperbranched polyurethane was carried out by an "A_2 + B_3" approach (Scheme 1). PCL based -NCO terminated prepolymer or excess MDI as A_2 monomer and triethanolamine as B_3 monomer were then used to prepare thermoplastic polyurethane. Different weight percentage of f-GO was incorporated in the second stage of the reaction for partially grafting of GO with HPU. The addition of highly functionalized aliphatic hydroxyl group containing f-GO and triethanolamine at low temperature and high dilution was also used to avoid gel formation. The composites are soluble in highly polar organic solvents, such as N,N-dimethylformamide, N,N-dimethylacetamine, 1-methyl-2-pyrrolidinone, and dimethyl sulfoxide, and can softened or hardened by varying the temperature. These results indicate that the GO grafted polymers are not gel type products and are thermoplastic in nature.

The FT-IR spectra (Fig. 2a) were analyzed for the structural analysis and completion of synthesized hyperbranched polyurethane composites (NHPU) with different wt% f-GO. The absorption band at 2250-2270 cm^{-1}, due to the -NCO group was disappeared, confirming the successful completion of the reaction. In Fig. 2a, the IR peaks at 1650 and 1725 cm^{-1} correspond to C=C and ester stretching, respectively, and the peaks at 2930 and 2860 cm^{-1} are due to aliphatic -C-H stretching.[22] The peaks at 1500-1575 cm^{-1} are due to -N-H stretching. The peaks at 1100-1250 cm^{-1} indicate the presence of -C-O-C in the ester and urethane.

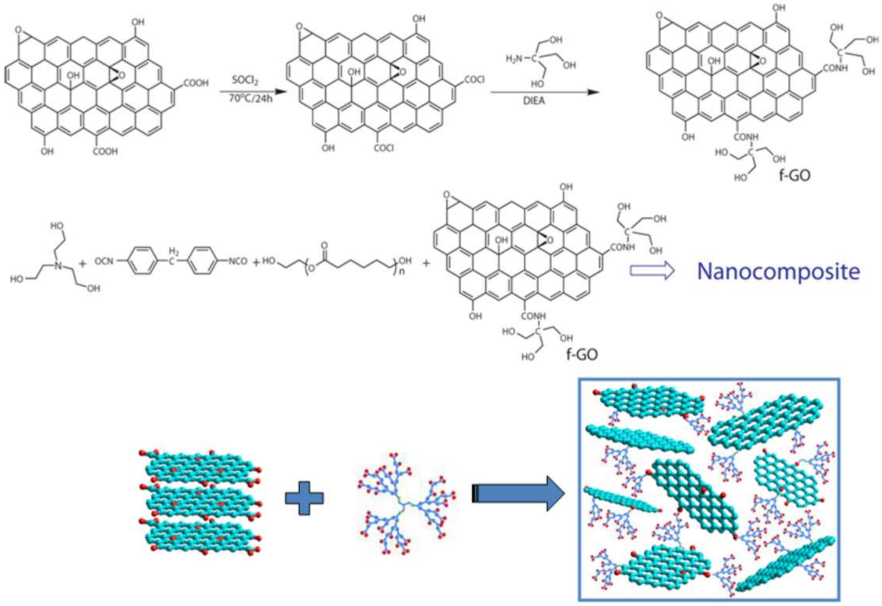

Scheme 1. Schematic representation of the synthesis of the graphene sheet grafted hyperbranched polymer.

However, the HPU-g-GO showed better dispersion in the DMF solution even after one week relative to pure GO and pristine GO/HPU nanocomposites. This may be due to the grafting of hyperbranched polymer on GO surface, which facilitates greater stability and solubility in an organic solvent. The success of HPU grafting from GO surface was confirmed by the evidence obtained by ^{1}H-NMR, TEM, and TGA analysis. The ^{1}H-NMR spectra (Fig. 2b) of the resulting HPU-g-GO confirmed the formation of polyurethane attachment on GO surface. The terminal OH and secondary -NH protons appeared at δ=9.6-9.4 and δ=8.7-8.5 ppm, respectively.[22] The aliphatic -CH$_2$ protons appeared at δ=5.1-1.2 ppm due to different chemical environment. The protons for the aromatic moieties form MDI appeared at δ = 7.33-7.01 ppm as a multiplet. Comparing with NHPU, the spectra of HPU-g-GO are well agreement with hyperbranched polyurethane structure.

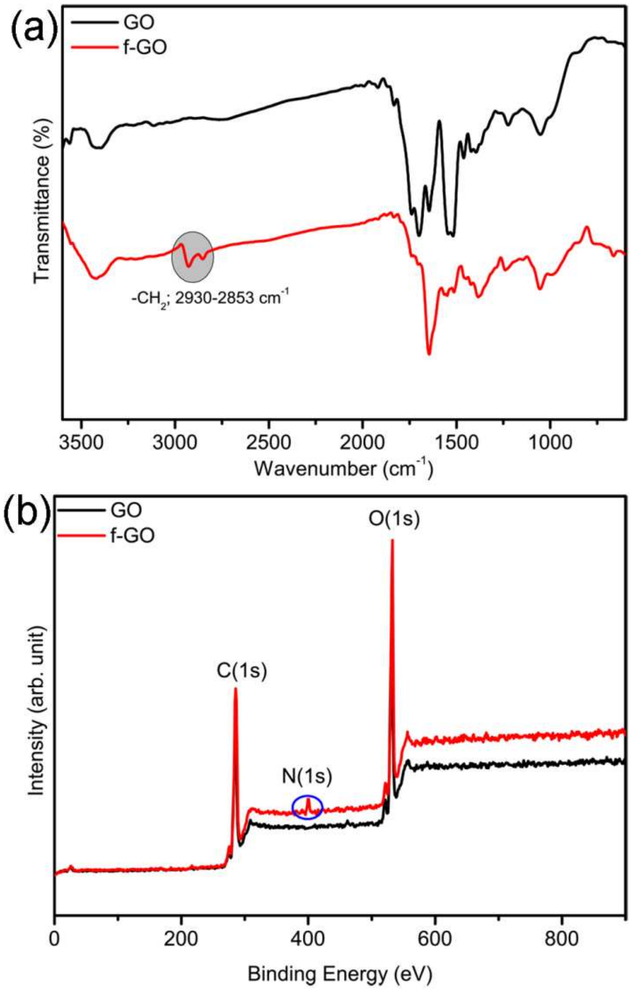

Fig. 1. (a) FT-IR and (b) XPS spectra of GO and f-GO.

To microscopically observe the sheet structure and morphology of GO sheets and HPU-g-GO for investigating the functionalization of HPU molecule on the graphene surface, TEM measurement was performed (Fig. 3). TEM results confirmed the existence of individual GO sheets in DMF. As shown in Fig. 3a, a typical TEM picture indicated that GO was fully exfoliated into individual sheets by ultrasonic treatment. In contrast, the image of HPU-g-GO is entirely different, which is shown in Fig. 3(b-d). It can be clearly observed that the surface of graphene is covered by a thin coating, which is likely to be the grafted HPU polymers. Moreover, it is clear that the polymer covered the convoluted surfaces of the platelets and that graphene sheets were exfoliated into thin layers.

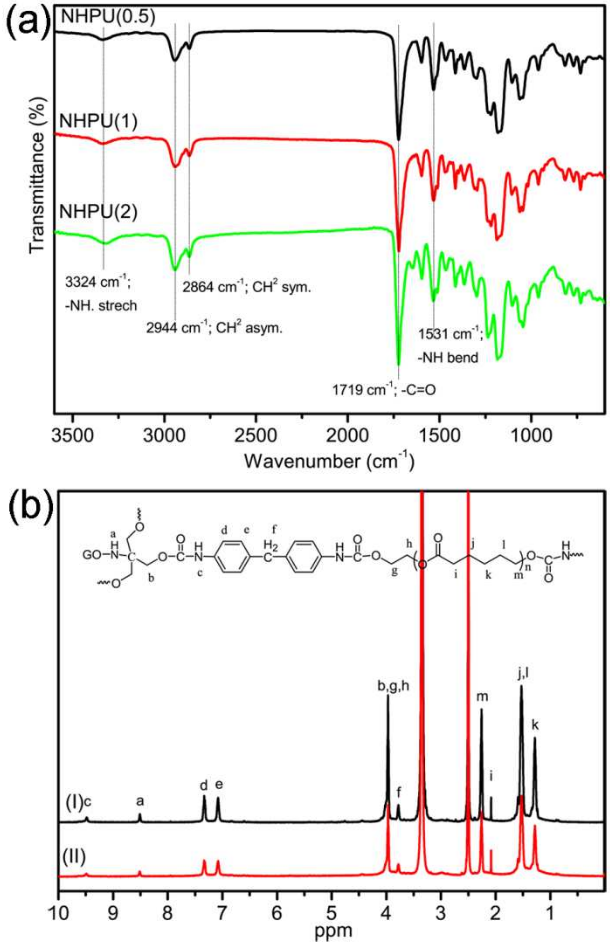

Fig. 2. (a) FT-IR of NHPU composites and (b) ^{1}H-NMR spectra of (I) NHPU(1) and (II) HPU-g-GO(1) composites.

Thermogravimetric analysis was employed to investigate the thermal stability of the materials. TGA plots of the GO and f-GO are shown in Fig. 4a. As for GO, the weight loss around 100 °C is ascribed to the evaporation of moisture from its layer structure,[29] and a significant weight loss can be found around 100-250 ^{o}C, which was caused by the decomposition of oxygen-containing functional groups such as hydroxyl, carboxyl and epoxy groups, demonstrating the deoxygenation of GO and inclination to reduced GO.[29] Different from GO, the f-GO is subject to a minor mass loss from about 100 °C, indicating that the oxygen-containing functional groups such as carboxyl and epoxy groups suggesting that the oxygen functional groups of GO have been removed during the functionalization. Generally, the reduction of the GO usually results in the high thermal stability due to the removal of the oxygen-containing functional groups. Thus, the thermal stability and the char residues of f-GO at 600 °C are improved, demonstrating that the GO has been partially reduced.[30] The implementation of covalent attachment between two phases affords good compatibility and even more uniform integration, which both can take advantage of the thermal stability of nanocomposites. The TGA curves of nanocomposites with different f-GO loadings are shown in Fig. 4b. It is clear that the thermal properties are significantly improved for nanocomposites containing f-GO, as compared to pure HPU. As for the thermal decomposition of polyurethane, the degradation starts after 300 ^{o}C and the does not release any volatile products below 300 °C. On incorporation of GO into the polyurethane matrix, the initial degradation temperature was increased significantly as shown in Fig. 4b (inset). As an example, at loading of 1.0 wt.% f-GO, the thermostability at 60 wt.% of NHPU(1) nanocomposites increased from 365 °C to 375 °C (increased by about 10 °C), indicating that the thermal stability of polyurethane is enhanced by functionalization with graphene sheets. In summary, it is expected that the thermal performance of the nanocomposites can be enhanced by the large aspect ratios of the graphene sheets, molecular-level dispersion in polyurethane matrix acted as a barriers, so-called “tortuous path” effect to prevent the permeation of oxygen, and the escape of volatile degradation products and also char formation.[31,32] The carbon surface of graphene nanofillers in the nanocomposites may act as a radical scavenger, resulting in delayed onset of thermal degradation.

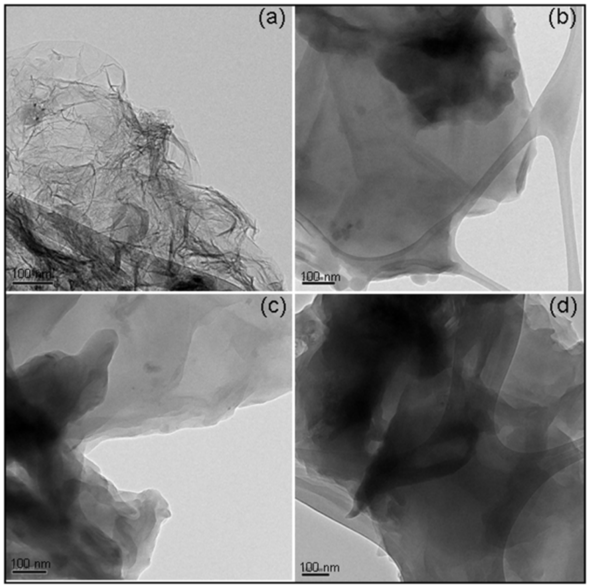

Fig. 3. TEM images of (a) GO, (b) HPU-g-GO(0.5), (c) HPU-g-GO(1), and (d) HPU-g-GO(2), respectively.

For shape memory polymers such as segmented polyurethane, the crystallization and melting behaviors are the key factor to their performances. In order to determine the role of graphene sheets and its content in the melting and crystallization behavior of NHPU nanocomposites, DSC thermal analysis studies have been performed. Fig. 5(a,b) represents the DSC cooling and second heating curves of the pure HPU and nanocomposites. It can be seen from Fig. 5a that the neat HPU and all the nanocomposites have only one exothermic peak, but the incorporation of f-GO sheets leads to a considerable increase in crystallization temperature (T_c) of the soft segments, implying that the well dispersed graphene sheets act as nucleation agents during crystallization of HPU. Thus, the increase in T_c indicates a good chemical affinity and interaction between nanofillers and HPU.[33] Enhanced soft-segment crystallinity of NHPU nanocomposites are not only increases storage capacity of strain-induced energy but also determines the temperature for thermal-triggered shape recovery. Besides, there are no large shifts in melting temperature of soft segments, which is consistent with previous results of HPU with a low weight loading of carbon nanofillers.[34]

In order to prepare high-performance graphene polymer composites, well dispersed and high-quality graphene is not enough; another crucial problem is to strengthen the interfacial adhesion to achieve efficient load transfer between graphene and the polymer matrix. Fig. 6a shows stress-strain curves for pure HPU and NHPU composite films. Apparent differences were found in Young’s modulus, tensile strength, and elongation-at-break point of the films as listed in Table 1. Compared with the pure HPU film, the tensile strength of the nanocomposite films, containing 1 wt.% graphene, increased by 18 % from 25.9 to 30.8 MPa, and Young’s modulus increased by 15.9 % from 81.3 to 94.2 MPa. Interestingly, up to 1 wt.% GO incorporated nanocomposites show excellent stretchability, as evidenced by the very high elongation-at-break. This may be because the presence of HPU chains on the surface of HPU-g-GO provides stronger interaction and interlocking in the HPU matrix. Moreover, the obtained graphene after functionalization (HPU-g-GO) has free functional groups on the basal plane or edge, and such a drawback greatly influences the interlocking force, which leads to the extra reinforcement of NHPU composites. As a result, a more effective load transfer across the graphene-HPU interface is obtained, resulting in a significant increase of tensile mechanical properties. However, the elongation-at-break presents a slightly downward trend with higher f-GO content. Fortunately, the resulting NHPU(2) composite films still maintain relatively high elongation-at-break, indicating that the incorporation of a relatively high quantity of GO cannot hinder the flexibility of the resulting composite films. The remarkable mechanical improvement in this study can be attributed to the hyperbranched polymer assisted homogeneous dispersion of HPU-g-GO as well as to the good adhesion between the HPU-g-GO and the HPU matrix.

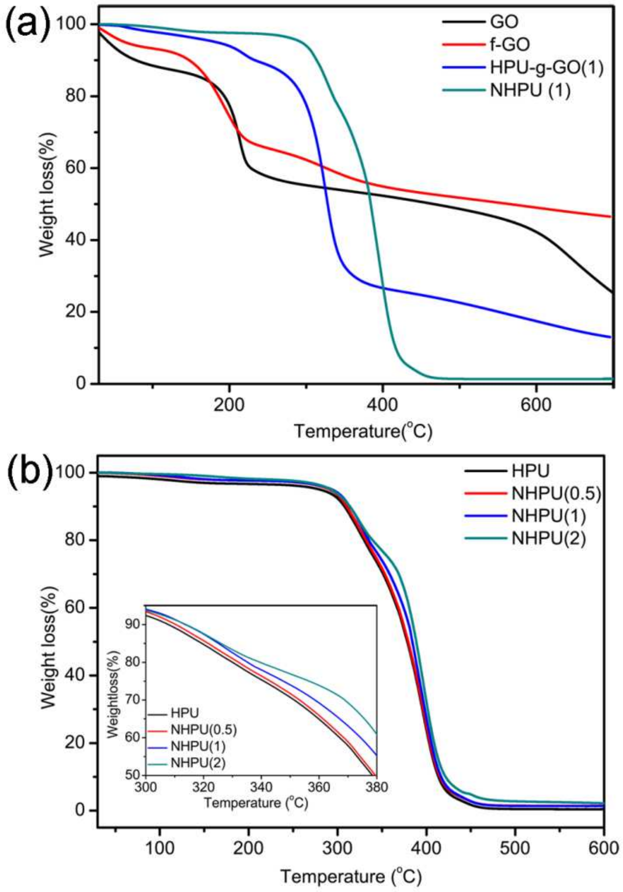

Fig. 4. TGA thermograms of (a) GO, f-GO, HPU-g-GO(1), and NHPU(1), and (b) pure HPU, and NHPU composites.

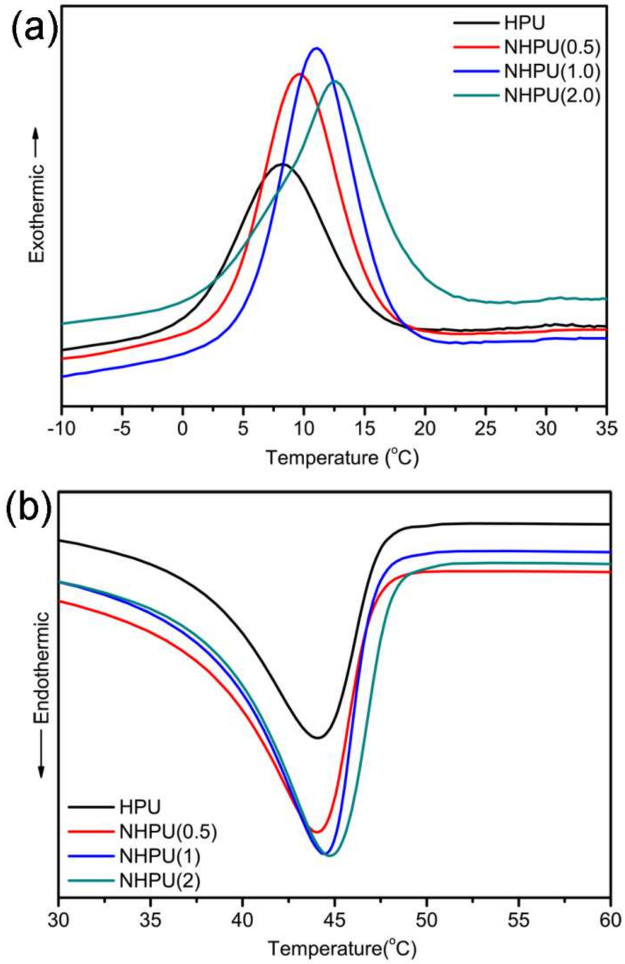

Fig. 5. (a) DSC thermograms measured on cooling from the melt and (b) its reheated curves for pure HPU and NHPU composites.

The thermo-responsive shape memory properties of the composites were analyzed (Fig. 6b). All the composite samples displayed higher than 95% shape retention and shape recovery as shown in Table 1. The NHPU composites exhibited better shape memory than the pure HPU. This may be due to good dispersion and higher compatibility of the nanofillers in the HPU matrix, which aids in obtaining higher recovery owing to the release of stored elastic strain energy.[35] The high surface area GO nanofillers could generate a lot of stored elastic strain energy, which in turn allowed the nanocomposites to acquire higher recovery stress. With an increase of the wt.% of graphene sheets in the hyperbranched polymer matrix, the shape recovery was also found to be increased, which is more profound in the case of NHPU(2), which may be due to the increased intermolecular interactions between graphene and HPU.

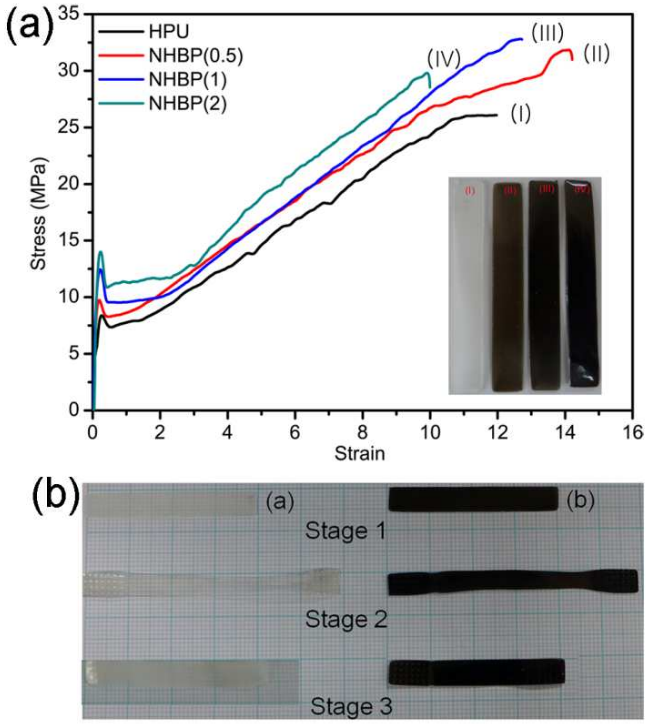

Fig. 6. (I) Stress–strain curves with the picture of composite films (inset): (i) pure HPU, (ii) NHPU(0.5), (iii) NHPU(1), and (iv) NHPU(2)), and (II) the representative samples during shape memory measurement of (a) pure HPU and (b) NHPU(1) composites, where stage 1, stage 2, and stage 3 indicate an initial, deformed (shape fixity), and final (shape recovery) stages, respectively.

4. Conclusions

A novel approach for the fabrication of high-performance hyperbranched polymer nanocomposites was demonstrated by using aliphatic hydroxyl group functionalized graphene sheets as an active reactant for in-situ polymerization. The graphene sheets were covalently functionalized with hyperbranched polyurethane to be well dispersed in a hyperbranched matrix and to simultaneously have strong interactions with the polymer matrix. It is believed that these composite films have potential applications as a shape memory material with enhanced strength.

Table 1. Mechanical and shape memory properties of pure HPU and NHPU composite films

Properties	HPU	NHPU(0.5)	NHPU(1)	NHPU(2)
Breaking stress (MPa)	25.9	30.8	31.7	29.7
Elongation-at-break (%)	11.9	14	12.6	9.9
Modulus (MPa)	81.3	94.2	112.3	118.6
Shape retention (%)	85	87	90	93
Shape recovery (%)	91	93	96	98

Acknowledgements

This work was supported by the National Research Foundation of Korea (NRF) grant funded by the Korea government (No. 2012R1A2A2A01015155) and 2013 KU brain pool of Konkuk University.

Notes and references

Department of Organic and Nano System Engineering, Konkuk University, Seoul 143-701, South Korea. E-mail: jwcho@konkuk.ac.kr; *Fax: +82-2-457-8895; Tel: +82-2-450-3513*

1. A. K. Geim, *Science,* 2009, **324**, 1530-1534.
2. M. J. Allen, V. C. Tung and R. B. Kaner, *Chem. Rev.,* 2010, **110**, 132-145.
3. R. Sengupta, M. Bhattacharya, S. Bandyopadhyay and A. K. Bhowmick, *Prog. Polym. Sci.*, 2011, **36**, 638-670.
4. T. Kuilla, S. Bhadra, D. Yao, N. H. Kim, S. Bose and J. H. Lee, *Prog. Polym Sci.* 2010, ***35***, 1350-1375.
5. X. L. Li, X. R. Wang, L. Zhang, S. W. Lee and H. J. Dai, *Science*, 2008, **319**, 1229-1232.
6. S. Stankovich, D. A. Dikin, G. H. B. Dommett, K. M. Kohlhaas, E. J. Zimney, E. A. Stach, R. D. Piner, S. T. Nguyen and R. S. Ruoff, *Nature*, 2006, **442**, 282-286.
7. D. Cai and M. Song, *J. Mater. Chem.,* 2010, **20**, 7906-15.
8. R. Verdejo, M. M. Bernal, L. J. Romasanta and M. A. Lopez-Manchado, *J. Mater. Chem.,* 2011, **21,** 3301-3310.
9. D. Chen, H. Feng and J. Li, *Chem. Rev*., 2012, **112**, 6027-6053.
10. H. Kim, A. A. Abdala and C. W. Macosko, *Macromolecules*, 2010, **43**, 6515–6530.
11. M. A. Rafiee, J. Rafiee, Z. Wang, H. Song, Z.-Z. Yu and N. Koratkar, *ACS Nano*, 2009, **3**, 3884-3890.
12. L. Q. Xu, L. Wang, B. Zhang, C. H. Lim, Y. Chen, K.G. Neoh, E. T. Kang and G. D. Fu, *Polymer*, 2011, **52**, 2376-2383.
13. Y. Xu, H. Bai, G. Lu, C. Li and G. Shi, *J. Am. Chem. Soc.,* 2008, **130**, 5856-5857.
14. S. Stankovich, D. A. Dikin, R. D. Piner, K. A. Kohlhaas, A. Kleinhammes, Y. Jia, Y. Wu, S. T. Nguyen and R. S. Ruoff, *Carbon,* 2007, **45**, 1558-1565.
15. H. J. Ryu, S. S. Mahapatra, S. K. Yadav and J. W. Cho, *Eur. Polym. Journal*, 2013, **49**, 2627-2634.
16. S. S. Mahapatra and N. Karak, *J. Appl. Polym. Sci.* 2007, **106**, 95-102.
17. Y. Zhou, W. Huang, J. Liu , X. Zhu and D. Yan., *Adv. Mater.*, 2010, **22**, 4567-4590.
18. C. Gao and D. Yan, *Prog. Polym. Sci.*, 2004, **29**, 183-275.
19. B. I. Voit and A. Lederer, *Chem. Rev.,* 2009, 109, 5924-73.
20. D. X. Zhuo, A. J. Gu, G. Z. Liang, J. T. Hu, L. Yuan and X. X. Chen, *J. Mater. Chem.*, 2011, **21**, 6584-6594.
21. S. S. Mahapatra, S. K. Yadav, H. J. Yoo and J. W. Cho, *J. Mater. Chem.,* 2011, **21**, 7686-7691.
22. S. S. Mahapatra, S. Rana and J.W. Cho, *J. Appl. Polym. Sci.,* 2011, **120**, 474-483.
23. X. Luo and P. T. Mather, *Soft Matter*, 2010, **6**, 2146-2149.
24. Y. C. Jung, H. J. Yoo, Y. A. Kim, J. W. Cho and M. Endo, *Carbon*, 2010, **48**, 1598-603.
25. Y. C. Jung, H. H. Kim, Y. A. Kim, J. H. Kim, J. W. Cho, M. Endo and M. S. Dresselhaus, *Macromolecules*, 2010, **43**, 6106-6112,
26. S. K. Yadav, H. J. Yoo and J. W. Cho, *J. Polym. Sci. Part B: Polym. Phys.,* 2013, **51**, 39-47.
27. S. S. Mahapatra, S. K. Yadav, H. J. Yoo, M. S. Ramasamy and J. W. Cho, *Sensor. Actuat. B - Chem.,* 2014, **193**, 384-390.
28. B. C. Chun, J. S. Park, C. H. Shin, J. W. Choi and B. C. Chun, *J. Macromol. Res.,* 2012, **20**, 66-75.
29. I. K. Moon, J. Lee, R. S. Ruoff and H. Lee, *Nat. Commun.,* 2010, **1**, 73-78.
30. S. Sun, Y. Cao, J. Feng and P. Wu, *J. Mater. Chem.,* 2010, **20**, 5605-5607
31. Y. W. Cao, Z. L. Lai, J. C. Feng and P. Y. Wu, *J. Mater. Chem.,* 2011, **21**, 9271-9278.
32. D. Y. Cai and M. Song, *J. Mater. Chem.,* 2010, **20**, 7906-7915.
33. Y. Feng, M. Qin, H. Guo, K. Yoshino and W. Feng, *ACS Appl. Mater. Interfaces*, 2013, **5**, 10882-10888.
34. S. K. Yadav, S. S. Mahapatra and J. W. Cho, *Polymer,* 2012, **53**, 2023-2031.
35. Q. Q. Ni, C. S. Zhang, Y. Fu, G. Dai and T. Kimura, *Compos. Struct.,* 2007, **81,** 176-184.

Table of Content (TOC)

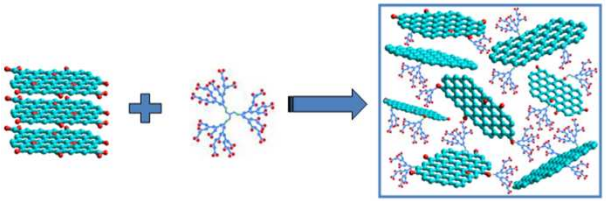

Covalently bonded graphene sheets with hyperbranched polyurethane were homogeneously dispersed in the matrix appeared as high performance shape memory material.